# Transcriptional Profiles in Nucleus Accumbens of Antidepressant Resistance in Chronically Stressed Mice

**Authors:**

Trevonn Gyles[1†], Eric M. Parise[1†], Molly S. Estill[1], Caleb J. Browne[1,2], Li Shen[1], Eric J. Nestler[1]*, Angélica Torres-Berrío[1,3,4]*

**Affiliations:**

[1]Nash Family Department of Neuroscience and Friedman Brain Institute, Icahn School of Medicine at Mount Sinai, New York, New York.

[2]The Centre for Addiction and Mental Health, Toronto, Canada

[3]Lurie Center for Autism, Massachusetts General Hospital, Boston, Massachusetts.

[4]Department of Pediatrics, Harvard Medical School, Boston, Massachusetts

***Corresponding author:**

eric.nestler@mssm.edu

atorres-berrio@mgh.harvard.edu

[†]These authors contributed equally to this work.

**ABSTRACT**

Unsuccessful response to several courses of antidepressants is a core feature of treatment-resistant depression (TRD), a severe condition that affects a third of patients with depression treated with conventional pharmacotherapy. However, the molecular mechanisms underlying TRD remain poorly understood. Here, we assessed the successful vs. unsuccessful response to ketamine (KET) in chronically stressed mice that failed to respond to initial treatment with fluoxetine (FLX) as a rodent model of TRD and characterized the associated transcriptional profiles in the nucleus accumbens (NAc) using RNA-sequencing. We observed that failed treatment with FLX exerts a priming effect that promotes behavioral and transcriptional responses to subsequent ketamine treatment. We also identified specific gene networks that are linked to both susceptibility to stress and resistance to antidepressant response. Collectively, these findings offer valuable insights into the molecular mechanisms underlying antidepressant resistance and help address a critical gap in preclinical models of TRD.

## INTRODUCTION

Unsuccessful response to several courses of antidepressants is a key signature of treatment-resistant depression (TRD), a serious subtype of major depressive disorder (MDD) that affects nearly 30% of patients treated with pharmacotherapy (*1-5*). While MDD is characterized by its high heterogeneity, with symptoms that vary according to severity and longitudinal trajectories (*6*), the lack of response to treatment despite adequate dose, duration, and adherence remains a significant challenge for clinical practice (*1, 5*). Unfortunately, the increased incidence of MDD as a direct consequence of the COVID-19 pandemic (*7*) and its leading contribution to the Global Burden of Disease during recent years highlight the urgent need to develop novel pharmacological approaches with better therapeutic outcomes (*7, 8*). A limitation to achieving this goal is the limited understanding of the neurobiology mediating successful versus unsuccessful responses to conventional therapies with currently available antidepressants.

In the clinic, conventional treatments for MDD have not evolved over the last several decades and continue to rely on pharmacological targeting of monoaminergic neurotransmission, such as selective serotonin reuptake inhibitors (SSRIs), serotonin and norepinephrine reuptake inhibitors (SNRIs), or tricyclic antidepressants (*9, 10*). These agents are the first-line choice for pharmacotherapy to treat MDD and are typically selected by trial-and-error or intuition of the treating professional (*9, 11*) due to the lack of reliable biomarkers or predictors of antidepressant efficacy (*12*). Nonetheless, virtually all classes of monoamine-based drugs have a delayed onset of therapeutic effects, requiring several weeks to display improvement of depressive symptomatology (*1, 13, 14*), and nearly half of the patients fail to achieve complete remission following a first option of pharmacotherapy (*1*); therefore, many patients need to undergo a second or third regimen of treatment (*1, 13*). More recently, Ketamine (KET), an antagonist of the glutamate N-methyl-D-aspartate (NMDA) receptor, among several other actions, has been shown to induce a rapid and lasting antidepressant response in

patients who have failed multiple treatments (*1, 15-18*), thus providing a novel non–monoamine-based therapeutic approach for MDD and TRD (*1, 15, 19-21*). Yet, KET is approved for use in TRD only, as it has not been approved as an initial choice to treat MDD (*18*). While the actions of conventional versus non-conventional treatments in alleviating depressive symptoms are continuously under investigation (*16-18*), the use of animal models has provided a valuable tool to study successful or unsuccessful responses to antidepressant treatments and may serve to identify mechanisms underlying treatment resistance (*12*). Unfortunately, most current preclinical studies using animal models focus on the antidepressant-like efficacy of a single course of treatment in drug-naïve animals, and many older studies relied on behavioral readouts that show robust responses to an acute dose of a conventional antidepressant, such as the forced swim test or tail suspension test. Thus, current models may not closely recapitulate the delayed response observed in humans following a chronic antidepressant regime (*22, 23*).

To develop a more comprehensive understanding of the molecular alterations related to treatment response versus non-response, our group previously analyzed broad transcriptional changes associated with antidepressant action using the chronic social defeat stress (CSDS) paradigm (*24*). CSDS is an extensively validated mouse model for the study of depression-like abnormalities (*25-27*) that separates mice into more susceptible versus more resilient populations based on a continuous distribution of responses in the social interaction test (SIT) (*25, 28, 29*). The SIT highly predicts many other, albeit not all, stress-induced behavioral abnormalities (*25, 28-30*) and is sensitive to the actions of chronic but not acute conventional antidepressant treatments or of single doses of ketamine (*27, 31*). Specifically, Bagot and colleagues (*24*) treated susceptible mice after CSDS with either chronic injections of the tricyclic antidepressant, imipramine, or a single injection of KET to profile gene expression changes associated with successful versus unsuccessful antidepressant responses in key regions of the limbic circuitry (*32-34*), including the nucleus accumbens (NAc), prefrontal cortex (PFC),

hippocampus (HPC), and amygdala (AMY), key regions of the brain's corticolimbic system that play a critical role in mood regulation (*32, 35*), and that are highly sensitive to the actions of antidepressants (*34*). Overall, this work demonstrated that successful response to either antidepressant was characterized by gene expression patterns resembling both pro-resilient and anti-susceptible transcriptional signatures (*24*). By contrast, unsuccessful response to either treatment associated with pro-susceptible gene expression patterns (*24, 36*), suggesting that aberrant transcriptional regulation may prevent the actions of antidepressants and, in turn, influence the likelihood of responding to a second round of treatment. A question that remains, however, is whether distinct transcriptional profiles are observed in mice that persistently fail to respond to multiple courses of antidepressant treatments and whether these transcriptional signatures could serve to uncover molecular mechanisms underlying TRD.

Here, we aimed to develop a novel paradigm of TRD in mice and characterize the transcriptional profile of successful versus unsuccessful responses to consecutive administration of antidepressants, with a focus on transcriptional responses in the NAc. For this purpose, mice deemed susceptible after CSDS and that failed to respond to an initial course of fluoxetine (FLX) treatment were further treated with a single injection of KET. We selected FLX because it is among the first-line SSRIs to treat MDD (*1, 14*), and it is tolerated especially well in mice when administered in drinking water (*37, 38*), which provides a more naturalistic and translational route of administration as compared to daily intraperitoneal injections of antidepressants (*39*). We found that prior failure of response to FLX promotes successful treatment with KET. We also identified a subset of mice that persistently failed to respond to consecutive FLX and KET treatment and uncovered genes signatures associated with treatment resistance to both drugs.

## RESULTS

### Response and Non-Response to Consecutive Courses of Antidepressant Treatments

To recapitulate unsuccessful responses to consecutive courses of antidepressant treatments in an attempt to model aspects of TRD, we subjected adult male mice to CSDS and separated mice into susceptible versus resilient populations based on a social interaction test (SIT) (*25, 26, 28, 29*). Mice exhibiting reduced social interaction in a first SIT (SIT1) were classified as susceptible and underwent antidepressant treatment with FLX (160 mg/L/day) in their drinking water for 28 days (SUS-FLX) or received regular drinking water during the same period (SUS-W) (Figure 1A-C). At the completion of the FLX regime, control, SUS-W, and SUS-FLX mice were assessed for antidepressant effects on a second SIT (SIT2). Overall, we observed that our FLX regime resulted in patterns of responders (FLX-RESP) versus non-responders (FLX-NR), with ~65% of FLX-treated mice displaying increased social interaction as compared to susceptible mice treated with water (Figure 1D-E), whereas the remaining 35% of FLX-treated mice continued to exhibit reduced social interaction (Figure 1D-E). These findings are roughly consistent with the patterns of response to FLX treatment observed in MDD patients (*1, 2*) and with previous studies showing variations in antidepressant responses in mice (*24, 25, 27, 40*). Importantly, these variations in treatment response were not due to differences in the amount of water consumed between the SUS-W, FLX-RESP, and FLX-NR groups (Figure 1F; Figure S1).

We next subjected mice that failed to respond to FLX (FLX-NR) and half of the susceptible mice treated with water (SUS-W) to a single injection of KET (10 mg/kg, IP) and assessed them in a third SIT (SIT3) 24 h after injection (Figure 1A-B). We observed that ~50% of susceptible mice that initially failed to respond to FLX showed increased social interaction after a single KET injection (FLX-NR/KET-RESP) (Figure 1G-H), while the remaining mice continued to display reduced social interaction (FLX-NR/KET-NR), suggesting that this latter subset of mice were resistant to the antidepressant actions of both FLX and KET (Figure 1G). Unexpectedly, none of

the susceptible mice treated with water responded to a single KET injection (SUS-KET-NR), which suggests that the antidepressant-like effects of KET become more effective after failed treatment with FLX. Together, our results demonstrate that susceptible mice exhibited variations in responses to consecutive antidepressant administration and highlights the utility of the CSDS paradigm to study TRD preclinically.

**Transcriptional Signatures in the NAc of Antidepressant Response Versus Non-Response**

The primary goal of this study was to generate transcriptional profiles associated with successful versus unsuccessful responses to consecutive courses of antidepressants in mice that are susceptible to CSDS (Figure 1A). We collected NAc tissue from non-stressed control mice, as well as susceptible mice that *(i)* were treated with plain water throughout the study (SUS-W), *(ii)* responded to an initial course of chronic FLX (FLX-RESP), *(iii)* failed to respond to FLX but displayed successful response to a subsequent single dose of KET (FLX-NR/KET-RESP, *(iv)* did not respond to consecutive courses of FLX and KET (FLX-NR/KET-NR), and *(v)* did not respond to a single injection of KET without prior FLX treatment (SUS-KET-NR) (Figure 1A-B), and processed it for RNA-sequencing. Analysis of the differentially expressed genes (DEGs) across groups compared to non-stressed controls identified the largest number of upregulated and downregulated genes in SUS-W mice (Down: 1907 and Up: 2572), followed by the FLX-RESP mice (Down: 705 and Up: 1156). We also observed a moderate number of DEGs in FLX-NR/KET-RESP (Down: 403 and Up: 760) and FLX-NR/KET-NR (Down: 510 and Up: 531) groups compared to controls (Figure 2A), while the SUS-KET-NR comparison displayed the lowest number of DEGs (Down: 390 and Up: 315). These results confirm that variations in the response to antidepressants associate differentially with gene regulation in the NAC of chronically-stressed mice (*24*).

We then used rank-rank hypergeometric overlap (RRHO), which enables us to compare transcriptional patterns genome-wide across experimental groups with non-stressed controls as a reference in a threshold-free manner (*41*). We first compared the transcriptional signatures of successful response to FLX (FLX-RESP) or lack of response to KET (SUS-KET-NR) compared to susceptible mice treated with water (SUS-W). We found a weak transcriptional similarity between the FLX-RESP and SUS-W mice (Figure 2B), while there was a greater gene overlap between SUS-KET-NR and SUS-W mice (Figure 2C). This finding suggests that a successful response to FLX is characterized by a reduction in the transcriptional alterations induced by CSDS. The fact that SUS-KET-NR mice show the lowest number of DEGs but exhibit a stronger concordance with the SUS-W group suggests that those genes that remain differentially expressed in the SUS-KET-NR group may capture the main drivers of susceptibility to CSDS (*24*).

Next, we compared the transcriptional signatures of successful or unsuccessful response to a consecutive course of antidepressants (FLX-NR/KET-RESP or FLX-NR/KET-NR) versus a single treatment (FLX-RESP or SUS-KET-NR) to determine whether FLX treatment primes transcriptional changes for a subsequent KET injection. Interestingly, we observed a strong transcriptional overlap among FLX-NR/KET-RESP or FLX-NR/KET-NR when compared to FLX-RESP (Figure 2D-E, Figure S2A-B), although the FLX-NR/KET-NR condition exhibited a trend for less concordance relative to FLX-RESP (Figure 2E, Figure S2B), which suggest that a subset of genes may drive unsuccessful response to antidepressants. By contrast, we found a weak transcriptional overlap between FLX-NR/KET-RESP and SUS-KET-NR (Figure 2F, Figure S2C), while more similarity was observed between FLX-NR/KET-NR and SUS-KET-NR (Figure 2G, Figure S2D). Collectively, these results demonstrate that chronic FLX administration induces stronger gene regulation in the NAc than a single KET treatment and indicate that FLX may prime both behavioral and transcriptional responses to subsequent KET treatment. The

concordance observed between the SUS-W, SUS-KET-NR, and FLX-NR/KET-NR groups warrants further investigation of this transcriptional signature denoting treatment non-response.

**Further Characterization of Transcriptional Signatures of Antidepressant Response Versus Non-Response**

Next, we sought to identify similarities in DEGs across individual monotherapy treatments. We visualized these similarities as a union heatmap with hierarchical clustering and performed a canonical pathway analysis (Figure 3A-B). First, we compared monotherapy treatment (SUS-KET-NR or FLX-RESP) to SUS-W. We observed that both KET and FLX treatments reversed the transcriptional changes observed in stress susceptible mice, even though the KET-NR mice did not show a behavioral response (Figure 1). This may underscore the interpretation that FLX treatment primes KET response as each drug induces partly similar transcriptional changes following monotherapy. To examine the similarities between response and lack of response to consecutive treatments of antidepressants we compared FLX-NR/KET-NR and FLX-NR/KET-RESP to FLX-RESP (Figure 3C-D). We observed that FLX-RESP had more transcriptional similarities to FLX-NR-KET-RESP, while FLX-NR-KET-NR seemed to have its own unique transcriptional profile that is inverse of the two.

To further classify DEGs observed between monotherapy and consecutive courses of antidepressants we utilized pattern analysis to identify unique gene expression signatures. When comparing monotherapy response versus non-response, we observed two patterns that represent non-response to KET (SUS-KET-NR), showing similar levels of expression across susceptible mice treated with water or KET (Figure 4A). Those same genes are also inversely expressed between control mice and mice that respond to FLX treatment. Moreover, we identified two patterns that uniquely capture FLX-RESP, which is comprised of genes that show similar expression between control mice and mice treated with FLX (Figure 4B). When

comparing response and non-response to consecutive treatments of antidepressants, we identified two patterns that captured the lack of response to FLX and KET (Figure 4C-D), which are comprised of genes that are uniquely up- or down-regulated in only the FLX-NR and SUS-KET-NR groups.

Together, these data show that response to FLX primes the NAc for KET treatment via unique regulation of gene expression. Following FLX priming, mice that respond to KET show strong transcriptional similarity to mice that respond to FLX alone. On the contrary, FLX-treated mice that fail to respond to KET display a unique transcriptional phenotype that is not like mice FLX or KET responders.

**Shared Transcriptional Organization in Stress Susceptibility and Resistance to Antidepressant Treatments**

Our findings suggest that unsuccessful response to antidepressants recapitulates aberrant transcriptional signatures of susceptibility to CSDS (*24*). We therefore hypothesized that the genes involved are organized into functional networks that subserve specific biological functions (*42, 43*). We applied multiscale embedded gene co-expression network analysis (MEGENA) (*42*), which allows defining gene clusters or modules that center around highly interconnected hub genes to construct an organized hierarchical network represented as sunburst plots (Figure 4A-E). We overlaid DEGs identified in the SUS-W relative to control comparison onto MEGENA networks to visualize the ways in which susceptibility to stress is coordinated across gene networks and experimental groups. We observed a primary enrichment for two upregulated gene networks in the SUS-W comparison (Figure 5A), specifically clusters 6 and 10, which largely persisted across SUS-KET-NR and FLX-NR/KET-NR comparisons (Figure 5B and 5E), but not in FLX-RESP or FLX-NR/KET-RESP groups, suggesting potential gene network

specifically associated with persistent susceptibility to stress or with lack of response to antidepressant treatments.

GO analysis of the genes included in cluster 6 highlighted biological processes involved in cellular metabolism and ATP synthesis (Figure 5F), in which genes previously implicated in depression, such as ATPase Secretory Pathway Ca2+ Transporting 2 (*Atp2c2*) and valosin-containing protein *(Vcp)* (*44, 45*). Interestingly, GO analysis of genes within cluster 10 identified biological processes associated with cholesterol and steroid metabolism (Figure 4G), including the low-density lipoprotein receptor (*Ldlr)*, mevalonate kinase (*Mvk)*, and HMG-CoA reductase *(Hmgcr)*, two pathways previously shown to be influenced by the actions of FLX and KET (*46, 47*), and that are affected in individuals with TRD (*47, 48*). Upon closer examination of the cluster 10 network structure to identify key hub genes that may drive antidepressant response, we observed a network with two densely populated gene clusters centered around synaptosomal-associated protein 25 (*Snap25)* and synaptogyrin 1 (*Syngr1),* genes with critical implications in membrane function of neurons and psychiatric disorders (*49, 50*). This network is uniquely upregulated for DEGs in the FLX-NR/KET-NR group, potentially driving antidepressant resistance in mice (Figure 6A-B, Figure S3A-E).

Collectively, our multiscale approach suggests that altered metabolic processes in conjunction with neuronal functions are potentially disrupted in antidepressant resistance and that an initial antidepressant regime induces plastic changes, even if unsuccessful behaviorally, that may prime future responses to subsequent treatment.

## DISCUSSION

Variations in the therapeutic effects of antidepressants despite adequate dose, duration, and adherence remain a significant challenge in clinical practice and may serve as a risk factor for TRD (*1-3, 5*). For decades, conventional pharmacotherapies for MDD have relied on mechanisms serendipitously identified more than 60 years ago; however, the alarming percentage of patients that need to undergo several courses of antidepressants before achieving improvement of symptoms underscores the urgent need to develop rapidly-acting treatments like KET with better therapeutic outcomes (*1-3, 5*). Using robust rodent stress models, such as CSDS, combined with consecutive courses of antidepressant treatments, offers a valuable strategy for modeling TRD in rodents and identifying novel targets for this condition. Here, we examined the successful versus unsuccessful responses to a single injection of KET in susceptible mice to CSDS that failed to respond to an initial course of FLX as a novel approach to model TRD in rodents. We also characterized the associated profiles of gene expression in the NAc, a key brain region implicated in MDD that is highly sensitive to the actions of antidepressants (*34*). Our multilevel transcriptional analysis revealed that an initial treatment with FLX primes gene regulation in the NAc that associates with greater transcriptional and behavioral responses to a subsequent injection of KET and unveiled a subset of NAc genes strongly linked to resistance to both drugs. Collectively, our study provides valuable insights into the molecular mechanisms that potentially underly TRD and addresses a critical gap in preclinical models, which focus on the variable efficacy of pharmacotherapies (*22, 23*) but do not typically assess the effects of consecutive antidepressant treatments.

At first glance, our behavioral results indicate that susceptible mice treated with FLX displayed the expected percentage of responders (65%) and non-responders (35%) to this drug, which recapitulates previous studies showing variations in responses to various antidepressants in stress-exposed mice (*24, 31, 51*). Likewise, our results are consistent with human studies

reporting diverse degrees of FLX efficacy in MDD-treated individuals (*1, 2*). Our results also showed that mice treated with KET following unsuccessful response to an initial course of FLX separated into responders (50%) and non-responders (50%). Strikingly, by contrast, we observed that none of the water-treated susceptible mice that received a single injection of KET showed an antidepressant-like effect to this drug. While previous evidence has shown that a single KET injection reverses social avoidance in nearly 50% of susceptible mice to CSDS with or without prior antidepressant treatment (*24, 51*), our new findings suggest that the rate of success of KET may be lower if the administration of this drug occurs longer after CSDS exposure (e.g., 2 weeks versus 4 weeks); therefore, aspects such as timing or treatment duration can impact the behavioral response to KET in mice. Moreover, this data further indicate that previous FLX administration, even if it fails to alleviate stress-induced behavioral abnormalities, may promote successful response to subsequent KET treatment. In this context, it would be critical to assess whether alternative antidepressant compounds (*52, 53*) or the combination of other types of conventional pharmacological treatments (*24*) produce parallel behavioral effects to those induced by FLX.

Robust evidence demonstrates that, while FLX and KET act initially on serotonin reuptake (*13, 34, 39*) and glutamate receptors (*15-18, 54*), respectively, both drugs eventually affect some common molecular pathways and initiate partly similar intracellular cascades that result in neuronal plasticity in the brain (*39, 55, 56*). Our transcriptional data indicate that response to FLX or to FLX/KET induced partly convergent gene regulation in the NAc, as evidenced by the high transcriptional overlap between mice that responded to FLX and those that failed to respond to an initial course of FLX but were subsequently treated with KET (Figure 2D-E). By contrast, this transcriptional overlap was attenuated in mice that were resistant to both FLX and KET (Figure 2E), indicating that, while FLX primed gene regulation in the NAc, the expression of a subset of FLX-induced genes varied according to the successful or unsuccessful response to

a second treatment with KET. This idea is further supported by the transcriptional concordance observed between water-treated susceptible mice that failed to respond to a single injection of KET and susceptible mice that were resistant to FLX and KET (Figure 2G). Therefore, we hypothesize that consecutive courses of antidepressants may trigger cumulative effects on specific signaling pathways that lead to distinct transcriptional programs and divergent behavioral and neuroplasticity outcomes.

MEGENA analysis identified two gene networks that were shared across SUS-W, SUS-KET-NR, and FLX-NR/KET-NR groups, an indication that unsuccessful response to antidepressants was characterized by persistent transcriptional signatures of stress susceptibility (*24*), which may prevent the therapeutic actions of antidepressants. In this context, we found networks enriched for genes involved in ATP synthesis (Figure 5F) and cholesterol and steroid metabolism (Figure 5G). Evidence shows that the expression of some of these genes is associated with symptoms of depression (*48, 57*) or influenced by the actions of FLX or KET *(46-48, 57-59)*, which altogether suggest that alterations in metabolic pathways may play significant roles in mediating the effects of antidepressants and determine susceptibility to TRD. In future experiments, we will experimentally manipulate the expression of genes associated with ATP or cholesterol metabolism within the NAc to test their contribution to antidepressant response (*59*). If this proves to be true, it might be possible to enhance the therapeutic efficacy of conventional antidepressant treatments by developing ways to reverse the molecular and, perhaps metabolic, adaptations of persistent susceptibility (*24*).

Closer visualization of gene networks identified *Snap-25* and *Syngr1* as potential key hub genes also associated with unsuccessful responses to antidepressants (Figure 6). SNAP-25 is a vital component of the SNARE complex, which is involved in releasing neurotransmitters for synaptic transmission (*60*) and has been implicated in psychiatric disorders, including depression (*49*), whereas SYNGR1 is a membrane protein associated with presynaptic vesicles

in neuronal cells (*60*), whose role has not been directly associated with depression but has previously been identified as a key hub gene in susceptible mice to CSDS (*61*). These findings imply that unsuccessful response to antidepressant treatments is characterized by changes in gene-to-gene interactions that can be visualized as a co-expression network involving both well-established and novel hub genes with functional roles in psychiatric disorders.

Despite its strengths, an important limitation of our study is its exclusive focus on male mice exposed to CSDS; thus, it is unclear whether the observed transcriptional profile of treatment resistance can be generalized to females. This is a timely and critical point given the higher prevalence of depression among women compared to men (*62, 63*) and the influence of sex on stress response and antidepressant effects (*64-67*). Therefore, future research must incorporate male and female subjects for a more comprehensive view of TRD mechanisms. Another limitation is that our criteria to determine a successful or unsuccessful response to treatment was based on the traditional SIT, which has been widely used to segregate mice across the continuum of susceptibility and resilience after CSDS exposure (*26*). While social avoidance during the SIT highly correlates with other behavioral abnormalities, such as alterations in reward-related decision-making and higher-order cognitive tasks (*25, 28-30*), further studies will assess whether treatment-resistant mice also display behavioral and cognitive alterations observed in TRD human populations (*68, 69*). Given the versatility of the CSDS paradigm, a promising direction is to leverage machine learning approaches to classify complex behavioral phenotypes in sophisticated behavioral tasks or in home cage environments to enhance the translational value of our mouse model, enabling more nuanced measurements of stress and antidepressant responses (*51, 64, 70-74*).

This study is the first to characterize transcriptional changes in successful versus unsuccessful responses to consecutive antidepressant treatments in susceptible mice to chronic stress. By capturing the transcriptional heterogeneity of antidepressant response and providing

a valuable online resource, our work sets the basis for future mechanistic studies examining avenues for new pharmacological targets. As we continue improving the translation of preclinical findings, these advances will likely impact on how we view, treat, and predict TRD, reinforcing the importance of personalizing antidepressant testing and treatment strategies.

## ACKNOWLEDGEMENTS

Finding:

This work was supported by grants from NIMH (R01MH129306) and the Hope for Depression Research Foundation to EJN; the Robin Chemers Neustein Award, and the Friedman Brain Institute Innovation Award to ATB; and the Brain & Behavior Research Foundation Award to EMP (Grant 30609). ATB is supported by the Massachusetts General Hospital Lurie Center for Autism, Department of Pediatrics, and Center for Diversity and Inclusion.

Author contributions:

A.T.B., E.M.P. and E.J.N. designed the studies. A.T.B., E.M.P. and T.G. performed behavioral and sequencing experiments. T.G. and M.E. performed sequencing-based bioinformatics with input from L.S. A.T.B., T.G., E.M.P., and C.J.B. performed tissue collection. A.T.B., and E.J.N. wrote the manuscript. A.T.B. and E.J.N. supervised the project. All authors discussed the results and commented on and edited the manuscript.

Competing interests:

The authors declare no competing financial interests.

Data and materials availability:

All data needed to evaluate the conclusions in the paper are present in the paper and/or the Supplementary Materials. All RNAseq data reported in this study will be deposited publicly in the Gene Expression Omnibus upon manuscript acceptance. Other supporting scripts/code used in this study are available from the corresponding author upon request.

## REFERENCES


1. R. S. McIntyre *et al.*, Treatment-resistant depression: definition, prevalence, detection, management, and investigational interventions. *World Psychiatry* **22**, 394-412 (2023).
2. A. J. Rush *et al.*, Acute and Longer-Term Outcomes in Depressed Outpatients Requiring One or Several Treatment Steps: A STAR*D Report. *American Journal of Psychiatry* **163**, 1905-1917 (2006).
3. T. B. Gibson *et al.*, Cost burden of treatment resistance in patients with depression. *Am J Manag Care* **16**, 370-377 (2010).
4. H. Akil *et al.*, Treatment resistant depression: A multi-scale, systems biology approach. *Neurosci Biobehav Rev* **84**, 272-288 (2018).
5. M. Fava, The challenges of defining and managing treatment-resistant depression in research and practice. *World Psychiatry* **22**, 350-351 (2023).
6. M.-H. Han, S. J. Russo, E. J. Nestler, in *Neurobiology of Depression,* J. Quevedo, A. F. Carvalho, C. A. Zarate, Eds. (Academic Press, 2019), pp. 123-136.
7. D. F. Santomauro *et al.*, Global prevalence and burden of depressive and anxiety disorders in 204 countries and territories in 2020 due to the COVID-19 pandemic. *The Lancet* **398**, 1700-1712 (2021).
8. G. M. D. Collaborators, Global, regional, and national burden of 12 mental disorders in 204 countries and territories, 1990-2019: a systematic analysis for the Global Burden of Disease Study 2019. *The Lancet Psychiatry* **9**, 137-150 (2022).
9. R. H. Perlis, Abandoning personalization to get to precision in the pharmacotherapy of depression. *World Psychiatry* **15**, 228-235 (2016).
10. A. Cipriani *et al.*, Comparative efficacy and acceptability of 21 antidepressant drugs for the acute treatment of adults with major depressive disorder: a systematic review and network meta-analysis. *Lancet* **391**, 1357-1366 (2018).
11. Z. D. Cohen, R. J. DeRubeis, Treatment Selection in Depression. *Annual Review of Clinical Psychology* **14**, 209-236 (2018).
12. T. M. Gyles, E. J. Nestler, E. M. Parise, Advancing preclinical chronic stress models to promote therapeutic discovery for human stress disorders. *Neuropsychopharmacology* **49**, 215-226 (2024).
13. A. A. Nierenberg *et al.*, Timing of Onset of Antidepressant Response With Fluoxetine Treatment. *American Journal of Psychiatry* **157**, 1423-1428 (2000).
14. C. N. Karson *et al.*, Human brain fluoxetine concentrations. *J Neuropsychiatry Clin Neurosci* **5**, 322-329 (1993).
15. C. A. Zarate Jr, M. J. Niciu, Ketamine for depression: evidence, challenges and promise. *World Psychiatry* **14**, 348-350 (2015).
16. P. Zanos, T. D. Gould, Mechanisms of ketamine action as an antidepressant. *Molecular Psychiatry* **23**, 801-811 (2018).
17. J.-W. Kim, K. Suzuki, E. T. Kavalali, L. M. Monteggia, Ketamine: Mechanisms and Relevance to Treatment of Depression. *Annual Review of Medicine* **75**, 129-143 (2024).
18. L. M. Riggs, T. D. Gould, Ketamine and the Future of Rapid-Acting Antidepressants. *Annual Review of Clinical Psychology* **17**, 207-231 (2021).
19. R. M. Berman *et al.*, Antidepressant effects of ketamine in depressed patients. *Biological Psychiatry* **47**, 351-354 (2000).
20. C. A. Zarate, Jr *et al.*, A Randomized Trial of an N-methyl-D-aspartate Antagonist in Treatment-Resistant Major Depression. *Archives of General Psychiatry* **63**, 856-864 (2006).
21. A. Aguilar-Valles *et al.*, Translational control of depression-like behavior via phosphorylation of eukaryotic translation initiation factor 4E. *Nature Communications* **9**, 2459 (2018).

22. B. J. Caldarone, V. Zachariou, S. L. King, Rodent models of treatment-resistant depression. *European Journal of Pharmacology* **753**, 51-65 (2015).
23. P. Willner, C. Belzung, Treatment-resistant depression: are animal models of depression fit for purpose? *Psychopharmacology* **232**, 3473-3495 (2015).
24. R. C. Bagot *et al.*, Ketamine and Imipramine Reverse Transcriptional Signatures of Susceptibility and Induce Resilience-Specific Gene Expression Profiles. *Biological Psychiatry* **81**, 285-295 (2017).
25. V. Krishnan *et al.*, Molecular Adaptations Underlying Susceptibility and Resistance to Social Defeat in Brain Reward Regions. *Cell* **131**, 391-404 (2007).
26. S. A. Golden, H. E. Covington, O. Berton, S. J. Russo, A standardized protocol for repeated social defeat stress in mice. *Nature Protocols* **6**, 1183-1191 (2011).
27. O. Berton *et al.*, Essential Role of BDNF in the Mesolimbic Dopamine Pathway in Social Defeat Stress. *Science* **311**, 864-868 (2006).
28. A. Torres-Berrío *et al.*, Mono-methylation of lysine 27 at histone 3 confers lifelong susceptibility to stress. *Neuron* **112**, 2973-2989.e2910 (2024).
29. R. Durand-de Cuttoli *et al.*, A Double Hit of Social and Economic Stress in Mice Precipitates Changes in Decision-Making Strategies. *Biological Psychiatry* **96**, 67-78 (2024).
30. E. J. Nestler, S. J. Russo, Neurobiological basis of stress resilience. *Neuron* **112**, 1911-1929 (2024).
31. R. J. Donahue, J. W. Muschamp, S. J. Russo, E. J. Nestler, W. A. Carlezon, Effects of Striatal ΔFosB Overexpression and Ketamine on Social Defeat Stress–Induced Anhedonia in Mice. *Biological Psychiatry* **76**, 550-558 (2014).
32. S. J. Russo, E. J. Nestler, The brain reward circuitry in mood disorders. *Nature Reviews Neuroscience* **14**, 609-625 (2013).
33. K. J. Ressler, H. S. Mayberg, Targeting abnormal neural circuits in mood and anxiety disorders: from the laboratory to the clinic. *Nature Neuroscience* **10**, 1116-1124 (2007).
34. N. R. Bolo *et al.*, Brain Pharmacokinetics and Tissue Distribution In Vivo of Fluvoxamine and Fluoxetine by Fluorine Magnetic Resonance Spectroscopy. *Neuropsychopharmacology* **23**, 428-438 (2000).
35. S. B. Floresco, The Nucleus Accumbens: An Interface Between Cognition, Emotion, and Action. *Annual Review of Psychology* **66**, 25-52 (2015).
36. F. Duclot, M. Kabbaj, Comparative Transcriptomic Analysis of the Effects of Antidepressant Drugs in Stress-Susceptible Mice. *Biol Psychiatry* **81**, 278-279 (2017).
37. A. Al-Kachak *et al.*, Histone serotonylation in dorsal raphe nucleus contributes to stress- and antidepressant-mediated gene expression and behavior. *Nature Communications* **15**, 5042 (2024).
38. D. A. Connor, T. J. Gould, Chronic fluoxetine ameliorates adolescent chronic nicotine exposure-induced long-term adult deficits in trace conditioning. *Neuropharmacology* **125**, 272-283 (2017).
39. G. de Foubert *et al.*, Fluoxetine-induced change in rat brain expression of brain-derived neurotrophic factor varies depending on length of treatment. *Neuroscience* **128**, 597-604 (2004).
40. N. M. Tsankova *et al.*, Sustained hippocampal chromatin regulation in a mouse model of depression and antidepressant action. *Nature Neuroscience* **9**, 519-525 (2006).
41. S. B. Plaisier, R. Taschereau, J. A. Wong, T. G. Graeber, Rank-rank hypergeometric overlap: identification of statistically significant overlap between gene-expression signatures. *Nucleic Acids Res* **38**, e169 (2010).
42. W. M. Song, B. Zhang, Multiscale Embedded Gene Co-expression Network Analysis. *PLoS Comput Biol* **11**, e1004574 (2015).
43. C. J. Browne *et al.*, Transcriptional signatures of heroin intake and relapse throughout the brain reward circuitry in male mice. *Science Advances* **9**, eadg8558 (2023).

44. D. Martins-de-Souza, P. C. Guest, N. Vanattou-Saifoudine, H. Rahmoune, S. Bahn, Phosphoproteomic differences in major depressive disorder postmortem brains indicate effects on synaptic function. *European Archives of Psychiatry and Clinical Neuroscience* **262**, 657-666 (2012).
45. D. Martins-de-Souza *et al.*, Identification of proteomic signatures associated with depression and psychotic depression in post-mortem brains from major depression patients. *Translational Psychiatry* **2**, e87-e87 (2012).
46. D. P. Uzunov, T. B. Cooper, E. Costa, A. Guidotti, Fluoxetine-elicited changes in brain neurosteroid content measured by negative ion mass fragmentography. *Proceedings of the National Academy of Sciences* **93**, 12599-12604 (1996).
47. G. I. Papakostas *et al.*, Serum Cholesterol in Treatment-Resistant Depression. *Neuropsychobiology* **47**, 146-151 (2003).
48. J.-C. Jiang, C. Hu, A. M. McIntosh, S. Shah, Investigating the potential anti-depressive mechanisms of statins: a transcriptomic and Mendelian randomization analysis. *Translational Psychiatry* **13**, 110 (2023).
49. J. W. Kim *et al.*, Investigation of variation in SNAP-25 and ADHD and relationship to co-morbid major depressive disorder. *American Journal of Medical Genetics Part B: Neuropsychiatric Genetics* **144B**, 781-790 (2007).
50. R. Verma, S. Kubendran, S. K. Das, S. Jain, S. K. Brahmachari, SYNGR1 is associated with schizophrenia and bipolar disorder in southern India. *Journal of Human Genetics* **50**, 635-640 (2005).
51. Y. Y. van der Zee *et al.*, Blood miR-144-3p: a novel diagnostic and therapeutic tool for depression. *Molecular Psychiatry* **27**, 4536-4549 (2022).
52. N. Hesselgrave, T. A. Troppoli, A. B. Wulff, A. B. Cole, S. M. Thompson, Harnessing psilocybin: antidepressant-like behavioral and synaptic actions of psilocybin are independent of 5-HT2R activation in mice. *Proceedings of the National Academy of Sciences* **118**, e2022489118 (2021).
53. R. Yehuda, A. Lehrner, Psychedelic Therapy—A New Paradigm of Care for Mental Health. *JAMA* **330**, 813-814 (2023).
54. A. E. Autry *et al.*, NMDA receptor blockade at rest triggers rapid behavioural antidepressant responses. *Nature* **475**, 91-95 (2011).
55. P. C. Casarotto *et al.*, Antidepressant drugs act by directly binding to TRKB neurotrophin receptors. *Cell* **184**, 1299-1313.e1219 (2021).
56. C. R. A. F. Diniz *et al.*, Fluoxetine and Ketamine Enhance Extinction Memory and Brain Plasticity by Triggering the p75 Neurotrophin Receptor Proteolytic Pathway. *Biological Psychiatry*, (2024).
57. L. Feng, C.-H. Tan, R. A. Merchant, T.-P. Ng, Association between Depressive Symptoms and Use of HMG-CoA Reductase Inhibitors (Statins), Corticosteroids and Histamine H2 Receptor Antagonists in Community-Dwelling Older Persons. *Drugs & Aging* **25**, 795-805 (2008).
58. L. Chang *et al.*, Role of oxidative phosphorylation in the antidepressant effects of arketamine via the vagus nerve-dependent spleen-brain axis. *Neurobiology of Disease* **199**, 106573 (2024).
59. C. Biojone *et al.*, Mutation in the TRKB Cholesterol Recognition Site that blocks Antidepressant Binding does not Influence the Basal or BDNF-Stimulated Activation of TRKB. *Cellular and Molecular Neurobiology* **44**, 4 (2023).
60. T. C. Südhof, The synaptic vesicle cycle: a cascade of protein-protein interactions. *Nature* **375**, 645-653 (1995).
61. Rosemary C. Bagot *et al.*, Circuit-wide Transcriptional Profiling Reveals Brain Region-Specific Gene Networks Regulating Depression Susceptibility. *Neuron* **90**, 969-983 (2016).

62. L. S. Leach, H. Christensen, A. J. Mackinnon, T. D. Windsor, P. Butterworth, Gender differences in depression and anxiety across the adult lifespan: the role of psychosocial mediators. *Social Psychiatry and Psychiatric Epidemiology* **43**, 983-998 (2008).
63. R. C. Kessler, Epidemiology of women and depression. *Journal of Affective Disorders* **74**, 5-13 (2003).
64. O. Issler *et al.*, The long noncoding RNA FEDORA is a cell type– and sex-specific regulator of depression. *Science Advances* **8**, eabn9494 (2022).
65. O. Issler *et al.*, Sex-Specific Role for the Long Non-coding RNA LINC00473 in Depression. *Neuron* **106**, 912-926.e915 (2020).
66. B. Labonté *et al.*, Sex-specific transcriptional signatures in human depression. *Nature Medicine* **23**, 1102-1111 (2017).
67. E. M. Parise *et al.*, Sex-Specific Regulation of Stress Susceptibility by the Astrocytic Gene Htra1. *bioRxiv*, 2024.2004.2012.588724 (2024).
68. D. A. Pizzagalli, Frontocingulate Dysfunction in Depression: Toward Biomarkers of Treatment Response. *Neuropsychopharmacology* **36**, 183-206 (2011).
69. D. A. Pizzagalli *et al.*, Pretreatment Rostral Anterior Cingulate Cortex Theta Activity in Relation to Symptom Improvement in Depression: A Randomized Clinical Trial. *JAMA Psychiatry* **75**, 547-554 (2018).
70. A. Torres-Berrío *et al.*, miR-218 in Adolescence Predicts and Mediates Vulnerability to Stress. *Biological Psychiatry* **89**, 911-919 (2021).
71. A. Torres-Berrío *et al.*, MiR-218: a molecular switch and potential biomarker of susceptibility to stress. *Molecular Psychiatry* **25**, 951-964 (2020).
72. O. Issler *et al.*, MicroRNA 135 Is Essential for Chronic Stress Resiliency, Antidepressant Efficacy, and Intact Serotonergic Activity. *Neuron* **83**, 344-360 (2014).
73. J. P. Lopez *et al.*, MicroRNAs 146a/b-5 and 425-3p and 24-3p are markers of antidepressant response and regulate MAPK/Wnt-system genes. *Nature Communications* **8**, 15497 (2017).
74. R. Durand-de Cuttoli *et al.*, Distinct forms of regret linked to resilience versus susceptibility to stress are regulated by region-specific CREB function in mice. *Science Advances* **8**, eadd5579 (2022).
75. D. Kim, B. Langmead, S. L. Salzberg, HISAT: a fast spliced aligner with low memory requirements. *Nature Methods* **12**, 357-360 (2015).
76. M. I. Love, W. Huber, S. Anders, Moderated estimation of fold change and dispersion for RNA-seq data with DESeq2. *Genome Biology* **15**, 550 (2014).
77. S. X. Ge, D. Jung, R. Yao, ShinyGO: a graphical gene-set enrichment tool for animals and plants. *Bioinformatics* **36**, 2628-2629 (2019).

## FIGURE LEGENDS

**Figure 1. Successful versus unsuccessful response to consecutive courses of antidepressants in susceptible mice after CSDS. (A)** Schematic and timeline of the CSDS experiment and fluoxetine (FLX) and ketamine (KET) administration. **(B)** Experimental groups: Control (CON), Water-treated susceptible (SUS-W), KET-non-responders (SUS-KET-NR), FLX-treated susceptible (SUS-FLX), FLX-responders (FLX-RESP), FLX-non-responders (FLX-NR), FLX-non-responders/KET-responders (FLX-NR/KET-RESP), and FLX-non-responders/KET-non-responders (FLX-NR/KET-NR). **(C)** Social interaction test 1 (SIT1). Interaction ratio prior to FLX treatment: One-way ANOVA: $F_{(2,45)}= 54.24$; $p<0.0001$. Tukey's test: SUS-W and SUS-FLX different from CON, ****$p<0.0001$. **(D)** Percentage of responder (FLX-RESP) and non-responder (FLX-NR) mice to FLX treatment. **(E)** Percentage of change from social interaction test 1 to test 2. Left: Change in time of interaction with social target: One-way ANOVA: $F_{(2,40)}= 11.33$; $p<0.001$. Tukey's test: Increased interaction time in FLX-RESP compared to SUS-W (*$p<0.05$) and FLX-NR (*$p<0.05$). Right: Change in Interaction ratio: One-way ANOVA: $F_{(2,40)}= 19.32$; $p<0.0001$. Tukey's test: Increased ratio in FLX-RESP compared to SUS-W (***$p<0.001$) and FLX-NR (**$p<0.01$). **(F)** Average of total water consumption during FLX treatment. One-way ANOVA: $F_{(2,30)}= 54.24$; $p=0.26$. **(G)** Social interaction ratio across antidepressant treatments. Two-way ANOVA: Group: $F_{(3,48)}= 15.61$; $p<0.0001$; Social interaction test: $F_{(2,48)}= 6.79$; $p<0.01$; Group by Social interaction test interaction: $F_{(6,48)}= 12.51$; $p<0.0001$. Tukey's test: Increased interaction ratio in FLX-NR/KET-RESP compared to SIT 3 in SUS-W, SUS-KET-NR, and FLX-NR/KET-NR, ****$p<0.0001$, and compared to SIT1 and SIT2 in FLX-NR/KET-RESP, ***$p<0.0001$. **(H)**. Percentage of responders (FLX-NR/KET-RESP) and non-responders (FLX-NR/KET-NR) to KET treatment in mice that failed to respond to FLX. Data: mean ± SEM.

**Figure 2. Patterns of transcriptional regulation induced in the NAc according to antidepressant response. (A)** Number of downregulated (blue) and upregulated (yellow)

differentially expressed genes (DEGs) across experimental groups relative to non-stressed controls (CON). DEG criteria: $Log_2$(fold change) > |0.20|, nominal p-value <0.05 and false discovery rate <0.1. **(B-C)** Rank-rank hypergeometric overlap (RRHO) plots showing coordinated transcription between FLX-RESP vs. CON and SUS-W vs. CON **(B)** or SUS-KET-NR and SUS-W vs. CON **(C)**. **(D-E)** RRHO plots depicting transcriptional overlap between FLX-NR/KET-RESP vs. CON and FLX-RESP vs. CON **(D)** or FLX-NR/KET-NR vs. CON and FLX-RESP vs. CON **(E). (F-G)** RRHO plots showing coordinated transcription between FLX-NR/KET-RESP vs. CON and SUS-KET-NR vs. CON **(F)** or FLX-NR/KET-NR vs. CON and SUS-KET-NR vs. CON **(G).** Arrows within quadrants indicate directionality of transcriptional overlap and heat denotes strength of the overlap.

**Figure 3. Differential gene regulation in the NAc in response to FLX and KET treatments. (A)** Union heatmap of DEGs in SUS-W relative to CON (top row), ranked by hierarchical clustering from lowest (blue) to highest (yellow), and corresponding $Log_2$(fold change) gene expression, across SUS-KET-NR and FLX-RESP comparisons. Differential criteria: $Log_2$(fold change) > |0.20|, and p<0.05. **(B)** Top canonical pathways commonly regulated between SUS-W, SUS-KET-NR and FLX-RESP comparisons. **(C)** Union heatmap of DEGs in FLX-RESP relative to CON (top row), ranked by hierarchical clustering from lowest (blue) to highest (yellow), and corresponding $Log_2$(fold change) gene expression, across FLX-RESP, FLX-NR/KET-RESP and FLX-NR/KET-NR comparisons. Differential criteria: $Log_2$(fold change) > |0.20|, and p<0.05. **(D)** Top canonical pathways commonly regulated between FLX-RESP, FLX-NR/KET-RESP and FLX-NR/KET-NR comparisons.

**Figure 4. Pattern analysis of expressed genes in the NAc in response to antidepressant treatments. (A)** Expression patterns of multiple genes enriched in the SUS-KET-NR group versus CON, SUS-W, FLX-RESP groups. **(B)** Expression patterns of multiple genes enriched in the FLX-RESP group versus CON, SUS-W, FLX-RESP groups. **(C)** Expression patterns of

multiple genes enriched in the FLX-NR/KET-NR group versus FLX-RESP and FLX-NR/KET-RESP. **(D)** Expression patterns of multiple genes enriched that are non-specific to either FLX-RESP, FLX-NR/KET-RESP, and FLX-NR/KET-NR.

**Figure 5. Gene network architecture of fluoxetine- and ketamine-induced transcriptional regulation in the NAc.** Multiscale Embedded Gene Co-expression Network Analysis (MEGENA) sunburst plots depicting **(A)** SUS-W, **(B)** SUS-KET-NR, **(C)** FLX-RESP, **(D)** FLX-NR/KET-RESP, and **(E)** FLX-NR/KET-NR groups. Sunburst plots are centered around a ring divided into outward segments that represent progressively condensed networks that emphasize condition-specific DEG enrichment. Coloration of sunburst plot segments depicts significant enrichment of upregulated (yellow) or downregulated (blue) genes in particular networks. Modules highlighted with red boxes indicate those networks emphasized that are shared across experimental conditions. **(F)** GO analysis showing the predominant biological processes associated with MEGENA networks Cluster 6, which is uniquely modulated in SUS-W and FLX-NR/KET-NR. **(G)** GO analysis depicting the predominant biological processes associated with MEGENA networks Cluster 10, which is uniquely modulated in SUS-W, SUS-KET-NR, and FLX-NR/KET-NR.

**Figure 6. Visualization of gene networks that illustrate key hub genes in the NAc associated with antidepressant resistance. (A)** Network structure of cluster 10 showing defined hubs as diamonds and non-hub nodes as circles, both sized by degree of connections. Differentially expressed genes (>20% FC, $p<0.05$) from the SUS-W condition are overlaid onto the FLX-NR/KET-NR network (upregulated, yellow shading; no change, gray shading), demonstrating near complete activation of this network. The remaining networks are shown in Figure S3. **(B)** Network structure of cluster 10 in the FLX-NR/KET-RESP network demonstrating near complete inactivation of this network. The remaining networks are shown in Figure S3.

## SUPPLEMENTARY FIGURE LEGENDS

**Figure S1. Water consumption during FLX treatment. (A)** Two-days average water consumption across the 28 days of FLX treatment. Two-way ANOVA: Group: $F_{(2,264)}$= 11.20; p<0.0001; Day: $F_{(10,264)}$= 24.88; p<0.0001; Group by Day interaction: $F_{(20,264)}$= 0.5242; p=0.95. Tukey's test: Increased water consumption in FLX-RESP (*p<0.01) and FLX-NR (*p<0.05) on Day 1.

**Figure S2. Gene overlap in the NAc across FLX-RESP, FLX-NR/KET-RESP, and FLX-NR/KET-NR comparisons. Related to Rank-Rank Hypergeometric Overlap (RRHOs) maps shown in Figure 2. (A)** Venn diagram showing common upregulated genes n FLX-RESP vs CON and FLX-NR/KET-RESP vs CON. There is ~68% gene overlap. **(B)** Venn diagram shows common downregulated genes n FLX-RESP vs CON and FLX-NR/KET-RESP vs CON. There is ~63% gene overlap. **(C)** Venn diagram showing common upregulated genes n FLX-RESP vs CON and FLX-NR/KET-NR vs CON. There is ~58% gene overlap. **(D)** Venn diagram showing common downregulated genes n FLX-RESP vs CON and FLX-NR/KET-NR. There is ~51% gene overlap.

**Figure S3. Visualization of gene networks that illustrate key hub genes in the NAc associated with antidepressant resistance. Related to Figure 6. (A)** Network structure of cluster 10 showing defined hubs as diamonds and non-hub nodes as circles, both sized by degree of connections. Differentially expressed genes (>20% FC, p<0.05) from the SUS-W condition are overlaid onto **(B)** SUS-KET-NR, **(C)** FLX-RESP, **(D)** FLX-NR/KET-RESP, and **(E)** FLX-NR/KET-NR group networks (upregulated, yellow shading; no change, gray shading), demonstrating near complete activation of this network.

## Materials and Methods

### Animals

Experimental procedures were performed in accordance with the guidelines of the Institutional Animal Care and Use Committee (IACUC) at the Icahn School of Medicine at Mount Sinai. All male mice used in these studies were maintained on a 12-hour light-dark cycle (lights on at 7:00) with ad libitum access to food and water throughout the experiments. All data derived from animal studies were analyzed by an experimenter blind to the conditions.

Male C57BL/6J wild-type mice (Postnatal day, PND, 75±15, Jackson Laboratory) served as experimental subjects in the chronic social defeat stress paradigm. Male mice were group-housed before exposure to the stress and single-housed at the completion of the last defeat session and before the social interaction test (SIT). Animals were randomized for exposure to stress (e.g., one mouse from each cage was assigned to each experimental condition or treatment: control or manipulation). The order of the animals was further randomized prior to behavioral tests.

Male CD-1 retired breeder mice (≥3 months old) previously screened for aggressive behavior were used as social aggressors for male stress exposure. CD-1 mice were obtained from Charles River Laboratories and were single-housed throughout the study.

### Stress Paradigms and Behavioral Assessments

**Chronic Social Defeat Stress (CSDS):** CSDS was performed as in (*26*). Briefly, each adult male C57BL/6J experimental mouse was exposed to 5 minutes of physical aggression by a male CD-1 mouse. At the completion of the session, C57BL/6J experimental and CD-1 mice were housed overnight in a 2-compartment hamster cage and separated by a transparent divider with holes to provide sensory, but not physical, contact. The procedure was repeated for a total of 10 consecutive days, in which experimental mice faced a new aggressor every day.

Control C57BL/6J mice were housed in 2-compartment cages with a different cage-mate every day. The CSDS protocol was conducted during the light cycle, between 11:00 and 14:00.

**Social Interaction Test (SIT):** Twenty-four hours after the last session of CSDS, C57BL/6J experimental mice were assessed in the SIT. This test consisted of 2 sessions in which defeated, and control mice explored a squared-arena (44 x 44 cm) in the absence or presence of a novel aggressor CD-1 mouse (social target) for a period of 2.5 minutes each session. In the first session, an empty wire mesh enclosure 10 cm (length) × 6.5 cm (width) × 42 cm (height) was located against one of the walls of the arena to assess baseline exploration. In the second session, an unfamiliar CD-1 aggressor was placed inside the wire mesh enclosure. The area that surrounded the enclosure was designated as the social interaction zone (14 cm x 9 cm), whereas the corner areas of the walls opposite to the enclosure were designated as corners (9 x 9 cm) and represented the farthest point from the social interaction zone. The time (in seconds) of interaction with the social target was measured during both sessions. The social interaction ratio (time of interaction with social target present/the time in interaction zone with social target absent) was calculated to classify mice as susceptible (ratio□1) and resilient (ratio≥1) as in (*26*). This simple measure has been shown to correlate strongly with numerous other behavioral outcomes, including cognitive flexibility (*28*).

**Fluoxetine (FLX) Treatment**

Twenty-four hours after the SIT, mice displaying a susceptible phenotype (reduced interaction time with social target and ratio □1) were assigned to either oral FLX treatment (Spectrum Chemicals, New Brunswick, NJ, USA) or regular drinking water (vehicle) for four weeks. FLX was dissolved in regular drinking water at a 160mg/L concentration and delivered *ad libitum* through Black Light-Safe 50mL polypropylene conical tubes capped with rubber stopper. The concentration and route of FLX administration were selected based on previous evidence showing antidepressant effects (*37, 38*). Water-treated susceptible mice and control mice

received regular drinking water in the same type of Black Light-Safe conical tubes. FLX and regular drinking water consumption were measured and replaced every third day.

Twenty-four hours after the final day of FLX treatment, all mice were assessed on a second SIT (SIT2), as described above. Mice that spent more time interacting with the social target and displayed an increase of >25% in the interaction time during the SIT2 compared to the SIT1 were defined as “responders” to FLX. In contrast, mice that interacted less with the target following treatment during the SIT2 were classified as “non-responders”.

**Ketamine (KET) Treatment**

Twenty-four hours after the SIT2, susceptible mice that failed to respond to FLX treatment and a subset of water-treated susceptible mice received a single intraperitoneal injection of KET at a 10 mg/kg dose (*24*) and assessed on a third SIT (SIT3), as described above. All control mice and water-treated susceptible mice were also included for behavioral and downstream analysis.

**Tissue Dissection**

To profile global changes in resting-state gene expression following FLX and KET treatments, PFC and NAc tissue samples were collected twenty-four hours after the SIT3. In brief, all experimental mice were euthanized by rapid decapitation, brains were removed and cooled with ice-cold PBS prior to slicing on a pre-defined brain matrix. Unilateral PFC punches (12-gauge) and bilateral punches of the NAc (14-gauge) were taken from 1 mm coronal sections starting on approximately plate 15 of the Paxinos & Franklin mouse atlas, frozen immediately on dry ice, and stored at −80°C until further use.

**RNA Isolation, Library Preparation and RNA-Sequencing**

Total RNA was isolated from PFC and NAc tissue with the RNeasy Mini Kit, according to the manufacture’s guidelines (Qiagen, Germantown, MD, USA). All RNA samples were determined to have 260/280 and 260/230 values ≥1.8. RNA integrity (RIN) was assessed using an Agilent

2100 Bioanalyzer with the RNA 6000 Nano assay (Agilent, Lexington, MA, USA), and only samples with RIN values above 8 were used for RNA libraries.

Libraries were prepared using a 50 ng concentration of purified RNA with the TruSeq Stranded Total RNA with ribosomal RNA depletion (Illumina, San Diego, CA, USA), according to the instructions from the manufacturer. The libraries were size selected and purified using AMPure XP beads (Beckman Coulter, Brea, CA, USA), and concentrations were measured by the High Sensitivity DNA Bioanalyzer assay (Agilent, Lexington, MA, USA). Libraries were submitted to sequencing with GENEWIZ/AZENTA (South Plainfield, NJ, USA) on an Illumina NovaSeq 6000 System with a minimum depth of 40 million paired-end reads per sample.

**Analysis of RNA-Seq Data**

Quality control was performed using FASTQC software (https://github.com/shenlab-sinai/NGS-Data-Charmer). Raw sequencing reads underwent adapter trimming and were mapped to mm10 using HISAT (*75*), and count matrices were generated using the feature Counts function of the Subreads program (https://subread.sourceforge.net). For differential gene expression, raw reads were aligned to the mouse genome (mm10) and analyzed using the DESeq2 package (*76*). Genes with less than 10 counts in less than 5 samples were excluded from the analysis. The following cutoffs were applied to identify differentially expressed genes: [Log2(Fold Change)] >|0.20| and a <0.05 p-value significance cutoff. Volcano plots were generated using the R package "EnhancedVolcano". Genes included in analyses met a criterion of 30%-fold change and $P < 0.05$. Gene Ontology analysis was conducted with ShinyGO (*77*). The ontological categories for molecular function, cellular component and biological process were determined to be significant if they passed both the hypergeometric and binomial tests with a fold enrichment ≥1.5 and FDR Q<0.05. Significant GO terms with less than five genes were discarded.

**Pattern Analysis for Differential Expression**

The R package DEGreport was used for quality control and downstream analysis following differential expression. The variance stabilized normalized counts file from DESeq2 was subseted to contain only differentially expressed genes. The degPatterns function determines the sets of genes that exhibit similar expression patterns across sample groups by using a hierarchical clustering approach based on pair-wise correlations. This tree is then cut to generate clusters of genes with similar expression. This cutting takes place in a way that provides the maximum amount of diversity of clusters, meaning that the variability seen across clusters is higher than the variability observed within each cluster.

**Rank-rank Hypergeometric Overlap (RRHO)**

RRHO provides the ability to compare gene expression profiles of two conditions in a threshold-free manner to identify the degree and significance of overlap (*41*). RRHOs were generated to compare transcriptomic overlap across lists for two distinct experimental conditions. For example, FLX-RESP x SUS-W compares gene lists from FLX-RESP versus CON against gene lists from SUS-W versus CON. RRHO plots were generated using the RRHO2 package with default settings (github.com/RRHO2/RRHO2).

**Multiscale Embedded Gene Co-Expression Network Analysis (MEGENA)**

MEGENA was performed as described in (*42*) using the R package MEGENA (github.com/songw01/MEGENA). The analysis was performed on NAc and PFC samples separately. The input for MEGENA was a normalized counts matrix containing all experimental conditions. 37 samples were used to construct a MEGENA network for the NAc and PFC which resulted in 61,769 and 62,343 edges respectively. Modules with less than 50 genes were excluded from downstream analysis. Hub genes were identified using a combination of node strength and node degree with 5% false discovery rate (FDR). Enrichment p-values were calculated using Jaccard similarity coefficient using the R package Gene Overlap (https://github.com/shenlab-sinai/GeneOverlap).

## MEGENA Network Visualization

To visualize the MEGENA networks, we selected the top 25% of hub genes and used the igraph and ggraph packages in R to generate graphical representations. We applied the Fruchterman-Reingold layout algorithm, which uses an attractive force to draw connected hub genes closer together and a repulsive force between all pairs of hub genes. This approach positions nodes with stronger correlations closer, resulting in shorter edges for highly correlated gene pairs and producing a clear, interpretable layout of network structure and connectivity

## Gene Ontology (GO) Enrichment Analysis

Gene ontology (GO) enrichment analysis was conducted using the clusterProfiler R package, with the function enrichGO for overrepresentation analysis of biological processes (BP). We used the 2023 Gene Ontology Consortium database, targeting biological process terms. Results were visualized in R using the tidyverse package, allowing for clear depiction of enriched pathways and their statistical significance. This approach helped to identify and categorize the biological processes most relevant to the differential expression profiles observed across treatment conditions.

## Quantification and Statistical Analysis

Sample sizes (n) and statistical tests used are indicated in the figure legends. All values were represented mean ± S.E.M. Statistical analysis was performed using Graphpad Prism 6.0. A significance threshold of $\alpha<0.05$ was used in all the experiments. Statistical differences between two groups were analyzed with Student's t-tests with two-tailed analysis. Otherwise, one-way, two-way or three-way ANOVAs were performed, followed by Tukey's or Sidak's multiple comparison tests. Outliers were screened using the ROUT method. No statistical methods were used to determine the sample sizes, but the number of experimental subjects is similar to sample sizes routinely used in our laboratory and in the field for similar experiments. Data with

normal distribution, and similar variance were analyzed with parametric statistics. Otherwise, nonparametric statistics were applied.

# Figure 1

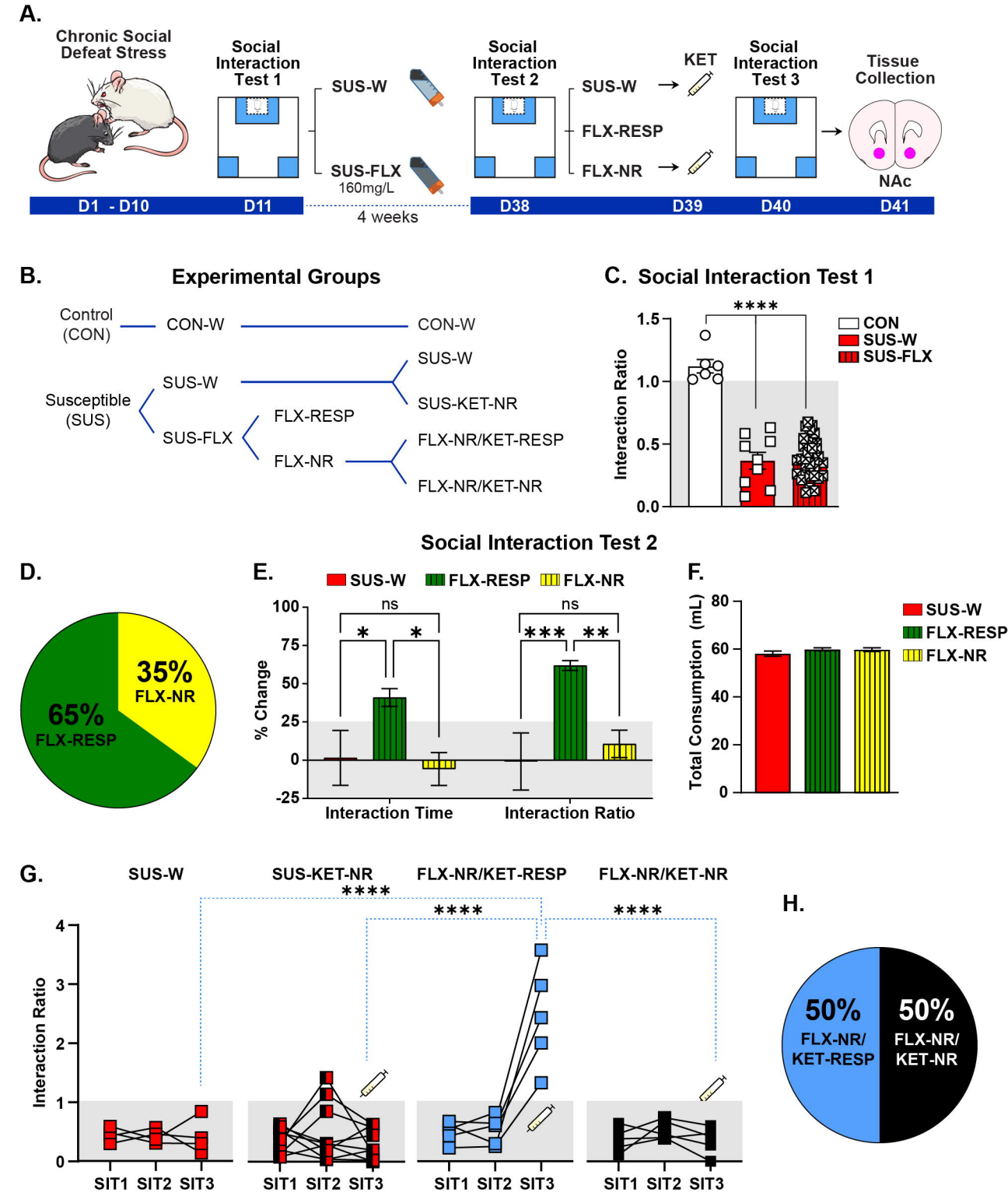
A.
Chronic Social Defeat Stress
Social Interaction Test 1
SUS-W
SUS-FLX
160mg/L
Social Interaction Test 2
SUS-W
FLX-RESP
FLX-NR
KET
Social Interaction Test 3
Tissue Collection
NAc
D1 - D10
D11
4 weeks
D38
D39
D40
D41
B.
Experimental Groups
Control (CON)
CON-W
CON-W
Susceptible (SUS)
SUS-W
SUS-W
SUS-KET-NR
SUS-FLX
FLX-RESP
FLX-NR
FLX-NR/KET-RESP
FLX-NR/KET-NR
C. Social Interaction Test 1
Interaction Ratio
CON
SUS-W
SUS-FLX
****
D.
35% FLX-NR
65% FLX-RESP
Social Interaction Test 2
E.
SUS-W
FLX-RESP
FLX-NR
% Change
ns
*
***
**
Interaction Time
Interaction Ratio
F.
Total Consumption (mL)
SUS-W
FLX-RESP
FLX-NR
G.
SUS-W
SUS-KET-NR
FLX-NR/KET-RESP
FLX-NR/KET-NR
Interaction Ratio
SIT1 SIT2 SIT3
H.
50% FLX-NR/ KET-RESP
50% FLX-NR/ KET-NR

# Figure 2

**A.**

| | DEGs relative to CON | |
|---|---|---|
| | Down | Up |
| SUS-W | 1907 | 2572 |
| SUS-KET-NR | 390 | 315 |
| FLX-RESP | 705 | 1156 |
| FLX-NR/KET-RESP | 403 | 760 |
| FLX-NR/KET-NR | 510 | 531 |

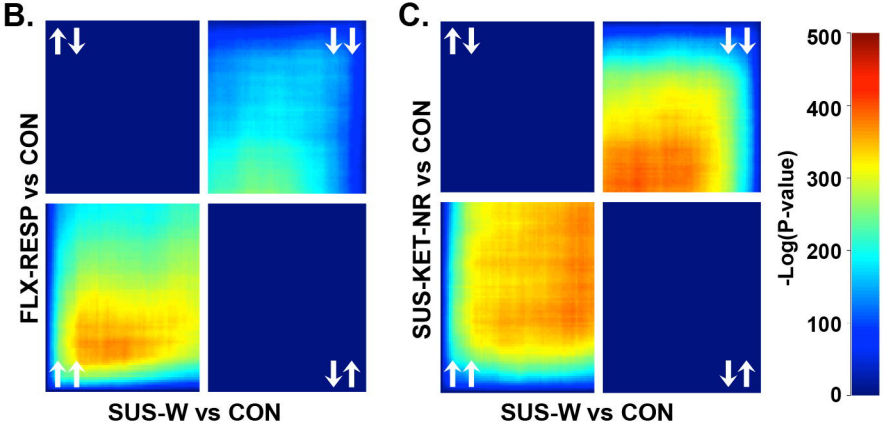


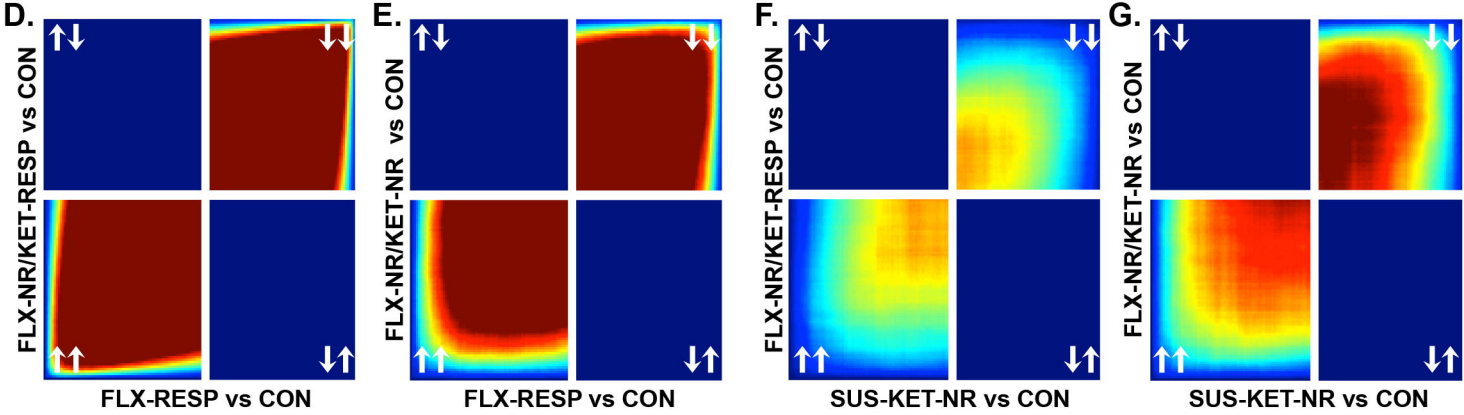

# Figure 3

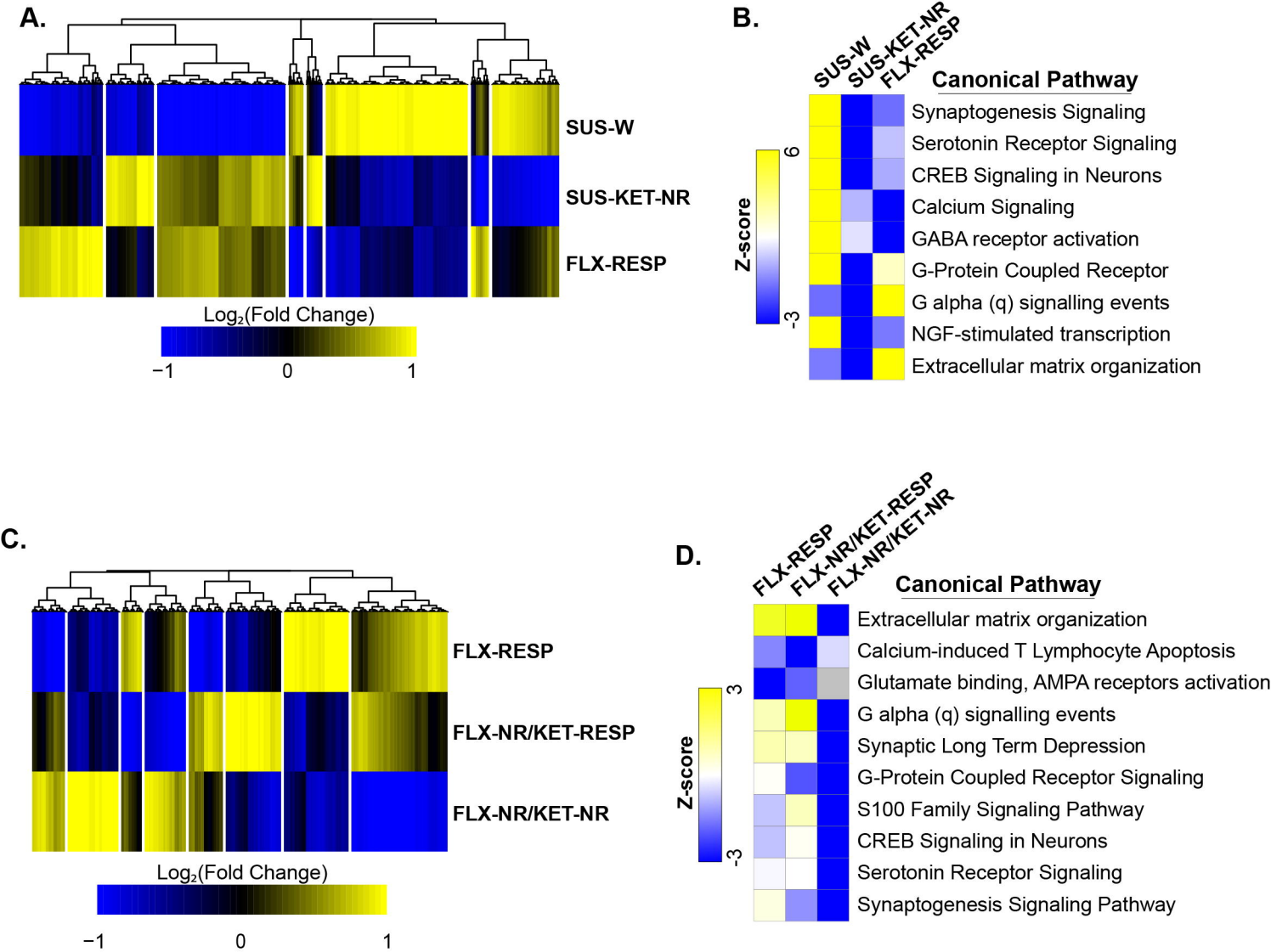
A.
SUS-W
SUS-KET-NR
FLX-RESP
Log2(Fold Change)
−1
0
1
B.
SUS-W
SUS-KET-NR
FLX-RESP
Canonical Pathway
Synaptogenesis Signaling
Serotonin Receptor Signaling
CREB Signaling in Neurons
Calcium Signaling
GABA receptor activation
G-Protein Coupled Receptor
G alpha (q) signalling events
NGF-stimulated transcription
Extracellular matrix organization
Z-score
6
-3
C.
FLX-RESP
FLX-NR/KET-RESP
FLX-NR/KET-NR
Log2(Fold Change)
−1
0
1
D.
FLX-RESP
FLX-NR/KET-RESP
FLX-NR/KET-NR
Canonical Pathway
Extracellular matrix organization
Calcium-induced T Lymphocyte Apoptosis
Glutamate binding, AMPA receptors activation
G alpha (q) signalling events
Synaptic Long Term Depression
G-Protein Coupled Receptor Signaling
S100 Family Signaling Pathway
CREB Signaling in Neurons
Serotonin Receptor Signaling
Synaptogenesis Signaling Pathway
Z-score
3
-3

# Figure 4

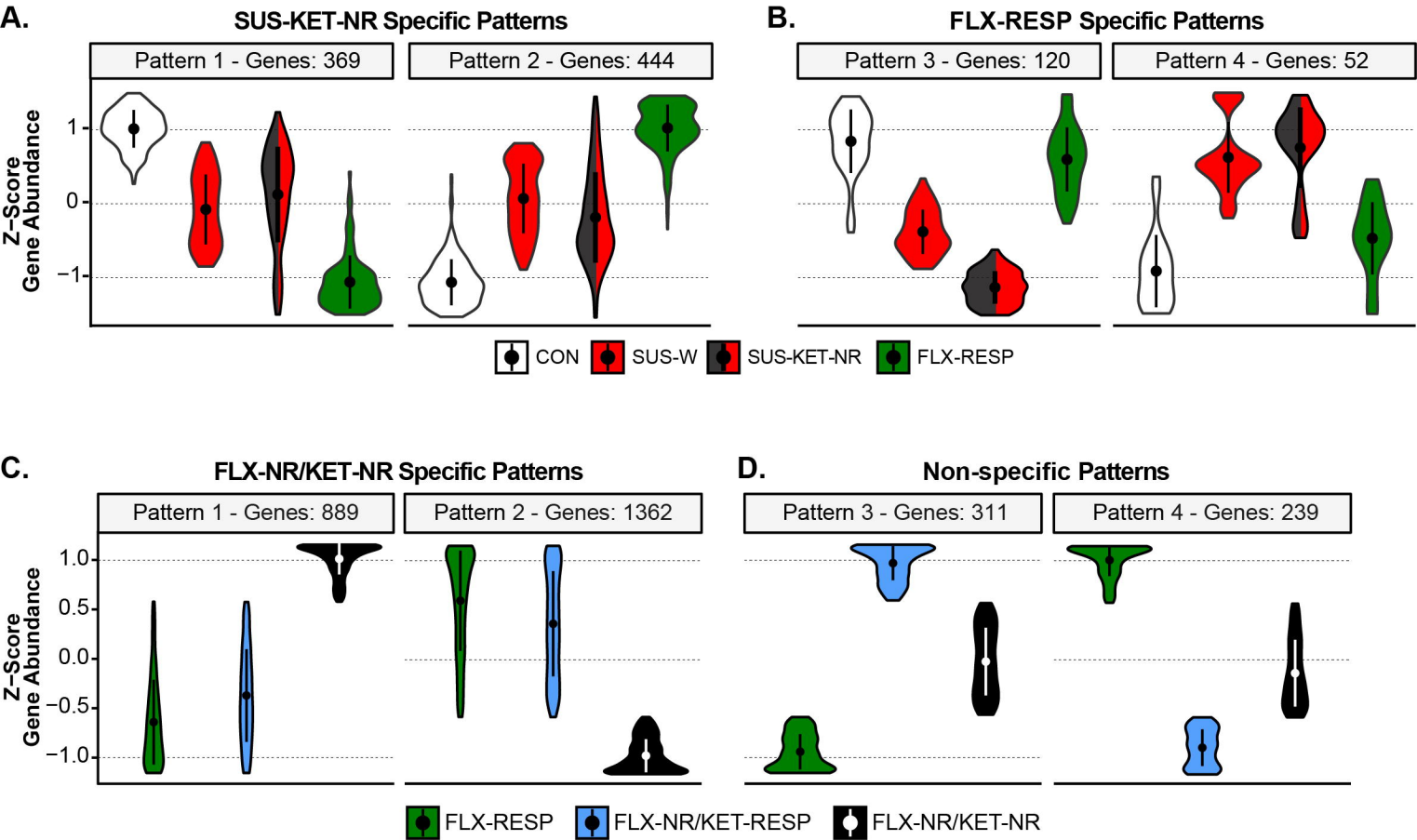
A.
SUS-KET-NR Specific Patterns
Pattern 1 - Genes: 369
Pattern 2 - Genes: 444
B.
FLX-RESP Specific Patterns
Pattern 3 - Genes: 120
Pattern 4 - Genes: 52
Z-Score
Gene Abundance
1
0
−1
CON
SUS-W
SUS-KET-NR
FLX-RESP
C.
FLX-NR/KET-NR Specific Patterns
Pattern 1 - Genes: 889
Pattern 2 - Genes: 1362
D.
Non-specific Patterns
Pattern 3 - Genes: 311
Pattern 4 - Genes: 239
Z-Score
Gene Abundance
1.0
0.5
0.0
−0.5
−1.0
FLX-RESP
FLX-NR/KET-RESP
FLX-NR/KET-NR

# Figure 5

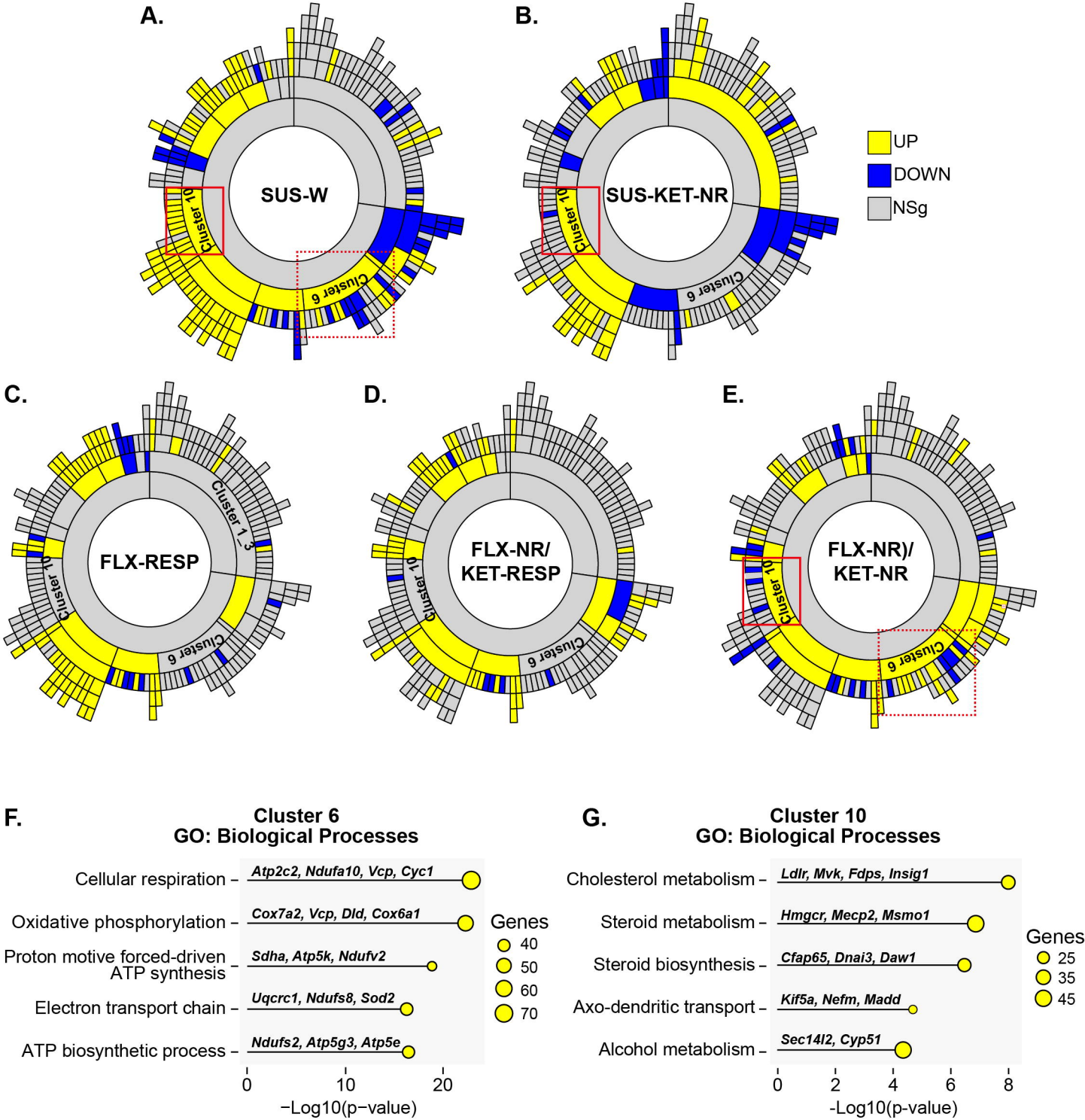
A.
SUS-W
Cluster 10
Cluster 6
B.
SUS-KET-NR
Cluster 10
Cluster 6
UP
DOWN
NSg
C.
FLX-RESP
Cluster 1_3
Cluster 10
Cluster 6
D.
FLX-NR/
KET-RESP
Cluster 10
Cluster 6
E.
FLX-NR)/
KET-NR
Cluster 10
Cluster 6
F.
Cluster 6
GO: Biological Processes
Cellular respiration
Atp2c2, Ndufa10, Vcp, Cyc1
Oxidative phosphorylation
Cox7a2, Vcp, Dld, Cox6a1
Proton motive forced-driven ATP synthesis
Sdha, Atp5k, Ndufv2
Electron transport chain
Uqcrc1, Ndufs8, Sod2
ATP biosynthetic process
Ndufs2, Atp5g3, Atp5e
Genes
40
50
60
70
0
10
20
−Log10(p−value)
G.
Cluster 10
GO: Biological Processes
Cholesterol metabolism
Ldlr, Mvk, Fdps, Insig1
Steroid metabolism
Hmgcr, Mecp2, Msmo1
Steroid biosynthesis
Cfap65, Dnai3, Daw1
Axo-dendritic transport
Kif5a, Nefm, Madd
Alcohol metabolism
Sec14l2, Cyp51
Genes
25
35
45
0
2
4
6
8
-Log10(p-value)

# Figure 6

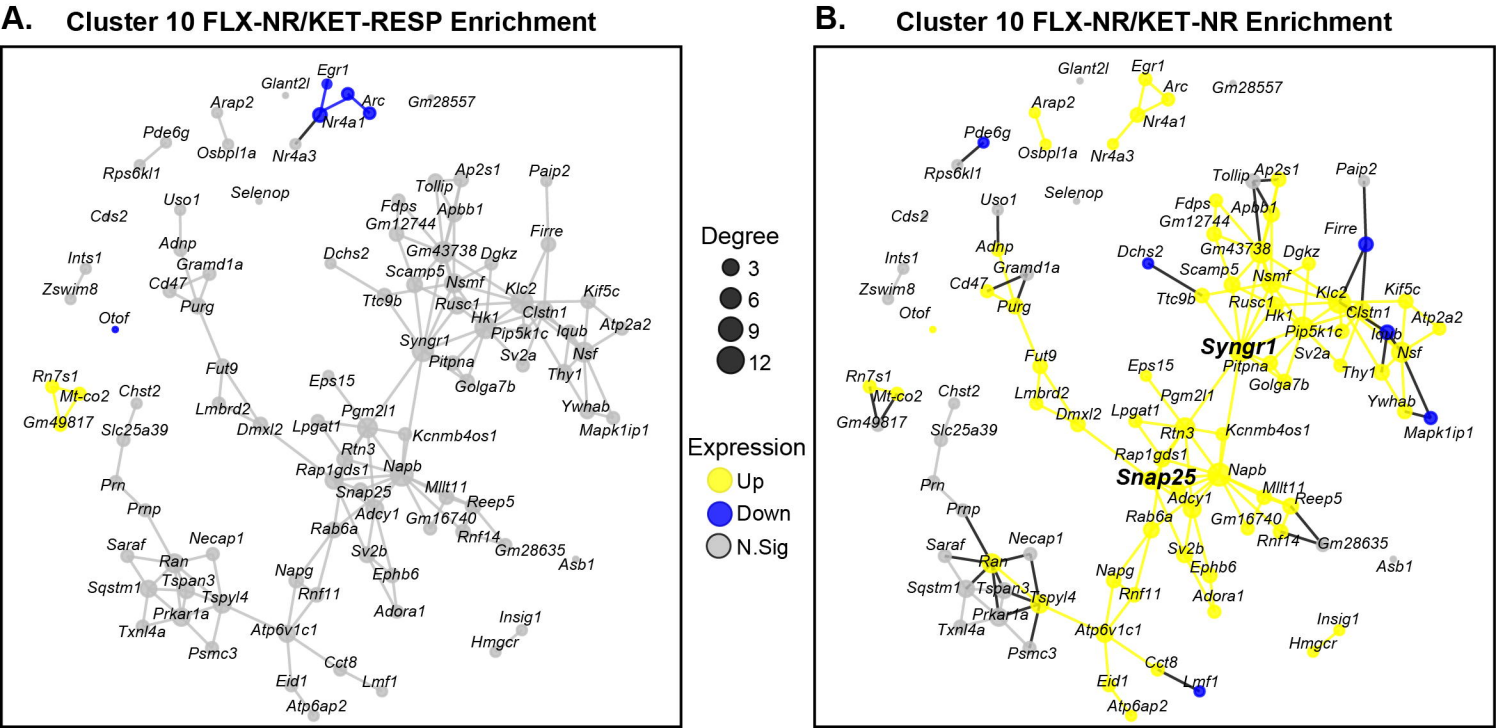
A.
Cluster 10 FLX-NR/KET-RESP Enrichment
B.
Cluster 10 FLX-NR/KET-NR Enrichment
Degree
3
6
9
12
Expression
Up
Down
N.Sig
Syngr1
Snap25